

# ***In vivo* evaluation of biocompatible intravascular stents coated by inkjet printing**

*Nicolaos Scoutaris<sup>1</sup>, Feng Chai<sup>2,3</sup>, Blandine Maurel<sup>2,3</sup>, Jonathan Sobocinski<sup>2,3</sup>, Min Zhao<sup>4</sup>,  
Jonathan G. Moffat<sup>4</sup>, Duncan Q. Craig<sup>4</sup>, Bernard Martel<sup>2,5</sup>, Nicolas Blanchemain<sup>2,3</sup>, Dennis  
Douroumis<sup>1\*</sup>*

<sup>1</sup> School of Sciences, Faculty of Engineering and Science, University of Greenwich, Medway, Kent, ME4 4TB, UK, <sup>2</sup> Université Lille Nord de France, 590000 Lille, France <sup>3</sup> INSERM U1008, Groupe Recherche Biomatériaux, Faculty of Medicine, Université Lille 2, Lille 59045, France, <sup>4</sup> UCL School of Pharmacy, University College London, 29–39 Brunswick Square, London WC1N 1AX, UK, <sup>5</sup>UMET CNRS 8207, Équipe Ingénierie des Systèmes Polymères, University Lille 1, 59655 Villeneuve d'Ascq – France

\*email: d.douroumis@greenwich.ac.uk

**Keywords:** drug eluting stents, inkjet printing, PLA, paclitaxel, simvastatin, cytokines, implantation

---

## **Abstract**

Inkjet–printing technology was used to apply biodegradable and biocompatible polymeric coatings of poly(D, L lactide) with the antiproliferative drugs simvastatin (SMV) and paclitaxel (PCX) on coronary metal stents. A piezoelectric dispenser applied coating patterns of very fine droplets (300 xL) and ink jetting was optimized to develop uniform, accurate and reproducible coatings of high yields on the stent strut. The drug loaded polymeric coatings were assed by scanning electron microscopy (SEM), atomic force microscopy (AFM) and transition thermal microscopy (TTM) where a phase separation was observed for SMV/PLA layers while PCX showed a uniform distribution within the polymer layers. Cytocompatibility studies of PLA coatings showed excellent cell adhesion with no decrease of cell viability and proliferation. In vivo stent implantation studies showed significant intra stent restenosis (ISR) for PXC/PLA and PLA plain coatings similar to marketed Presillion® (bare metal) and Cypher® (drug eluting) stents. The investigation of several cytokine levels after seven days of stent deployment showed no inflammatory response and hence no *in vivo* cytotoxicity related to PLA coatings. Inkjet printing can be employed as a robust coating technology for the development of drug eluting stents compared to the current conventional approaches.

**Keywords:** drug eluting stents, inkjet printing, PLA, paclitaxel, simvastatin, cytokines, implantation

## Introduction

In the last twenty years drug eluting stents (DES) have revolutionized interventional cardiology and have been widely adopted due to the improvements in angiographic and clinical outcomes.<sup>1, 2</sup> DES have shown better performance compared to bare metal stents (BMS) and demonstrated significantly lower late loss, target vessel, revascularization and major adverse cardiovascular events in follow up studies in 6 and 12 months.<sup>3</sup> Although the risks of mortality associated with DES and BMS has been shown to be similar the clinical effect of DES appears to be superior.<sup>4</sup>

For DES, an active pharmaceutical ingredient (API) along with a suitable polymer, which serves as a carrier to control the release of the drug, is coated on the stent strut. After implantation the API is released in order to inhibit neointimal cell formation, preventing thrombosis of the arteries. However, the first-generation DES incorporated non-erodible polymers, which were associated to increased risks of death, myocardial infarction, or stent thrombosis. In fact animal and human trials provided evidence of arterial inflammation, delayed vascular healing which subsequently led in precipitating stent thrombosis and delayed restenosis.<sup>5-8</sup> These findings stress the need for the development of biodegradable and more biocompatible polymer coatings, which eventually degrade in inert monomers and reduce the long-term risks. A wide range of materials has been developed to provide new novel DES by using PLGA grades,<sup>9</sup> poly-L-lactid acid (PLLA),<sup>10</sup> pullulan hydrogels,<sup>11</sup> polystyrene-binding peptides<sup>12</sup> and DNA-containing polyelectrolyte multilayers.<sup>13</sup> Several therapeutic agents including antiproliferative and immunosuppressive molecules demonstrated impressive clinical benefits such as sirolimus, everolimus, zotarolimus, paclitaxel and more recently biolimus. Simvastatin can reduce the Low Density Lipoprotein Cholesterol (LDL-C)<sup>14</sup> and it has been proved efficient to prevent neointimal formation with a positive effect in vascular smooth cell proliferation.<sup>15</sup>

Up to date, spray coating and dip coating have been reported as the main technologies to apply drug/polymer layers on the stent strut. In spray coating, a nozzle sprays a drug – polymer solution generating droplets of 10 – 15  $\mu\text{m}$  on a stent.<sup>16</sup> In the case of dip coating, the stent is deposited in the coating solution and subsequently spinned to remove the excess material. This process is repeated until the appropriate amount of drug is deposited.<sup>17</sup> However, the limitations of these techniques are related to the low yield and the time consuming processing. To overcome these drawbacks, inkjet printing technology may serve as an alternative approach to coat coronary stents. Inkjet printing is a non-contact technique that has been used to dispense pico-quantities of biologically related materials. In recent years, inkjet printing received increased attention in pharmaceutical and biomedical industry. It is a versatile technology and has been used for the development of various drug delivery systems such as polymeric microparticles with controlled dissolution profiles<sup>18</sup> oral films<sup>19</sup> coating of transdermal microneedles surfaces<sup>20</sup> and stents coating of drug loaded polymeric layers.<sup>21</sup> Inkjet printing has been used for stent coating due to the high reproducibility and accuracy while the capacity to follow patterns of stents with complex design can be proved advantageous. In addition, inkjet printing can significantly reduce material waste leading to high coating yields by controlling sample aspiration from the dispenser nozzle.

In inkjet printing, an acoustic pulse ejects droplets from a reservoir through the nozzle either by thermal heating or through a piezoelectric system. In thermal inkjet jetting (or bubble-jet) the solution in the dispenser is heated locally to form a rapidly expanding vapor bubble that ejects an ink droplet. Thermal jetting uses water as a solvent and may therefore impose restrictions on the selection of the drugs and polymers that can be printed, although non-aqueous thermal inks are available. Piezoelectric inkjet printing is based on the deformation of some piezoelectric material upon voltage appliance. Specifically, when voltage apply to the wall of a piezoelectric crystal, it changes its shape to a pre-ordained direction causing a

sudden volume change, creating pressure waves which results in a drop being ejected out of the orifice.

Here we report a feasibility study where inkjet-printing technology was used to apply biodegradable and biocompatible PXL/PLA and SMV/PLA coatings on stent struts. The uniform drug loaded polymeric layers were assessed both *in vitro* and *in vivo* for their cytotoxicity, biocompatibility and reduction of intra stent restenosis.

## **1. Materials – Methods**

### **Materials**

Simvastatin (SMV) and paclitaxel (PCX) were purchased from Sigma – Aldrich and from INRESA (Bartenheim, France). Poly(D, L lactide) (Resomer 205) was purchased from Evonic (Darmstadt, Germany). Dichloromethane (DCM) was purchased from Sigma-Aldrich (UK). Presillion<sup>®</sup> and Cypher<sup>®</sup> stents were donated from Abbott Vascular (Abbott, Rungis Cedex, France) and Cordis (Johnson & Johnson, Fremont, USA). For the *in vitro* biological evaluation studies, CoCr disks were cut into a cobalt–chromium rod (∅14.5 mm) according to ISO standards 5832-12 (Co 66.00%, Cr 27.34%, Mo 5.19%, Mn 0.56%, Si 0.39%) bought from Böhler-Edelstahl, Germany with a thickness of 3 mm each.

### **Ink jetting process for DES coating**

For the purposes of the studies ink jetting was conducted by using a Nanoplotter II from (GeSim GmbH, Dresden, Germany) fitted with a PicPip 300 dispenser. Solutions of drug and polymer were prepared by dissolving the compounds in DCM at a 1:3 (wt/wt) drug/polymer ratio (SMV/PLA, PXL/PLA). The technology dispenses and can accurately aspirate aqueous and organic solutions. The system consists of the wash station, the dispenser and the dispense

control system. The amount of aspiration is controlled via an accurate flow sensor while a stroboscope ensures that the dispenser ejects the droplets (Fig 1a). Stroboscopic image capture provides real-time analysis of pipette performance both before and after sample dispensing. Droplet diameter allows estimation of the dispensed volume calculated through image analysis. If, for any reason, a sample is not dispensed as instructed (e.g. empty sample well), the software logs this and allows for repetition of respective sample printing, thus ensuring completion of the task. If there is a failure in droplet ejection the nano-plotter will wash the microdispenser and repeat the sample aspiration.

The drug/polymer solutions were jetted through a piezodriven dispenser (PicPip 300) onto the stent strut in the form of fine droplets of approximately 300 pl whereas the stent was gripped on a rotating holder, which rotates in a control manner (Fig 1). The dispenser is a piezoelectric ceramic that is deformed upon voltage appliance, thus ejecting a droplet from the nozzle at a speed 1-5m/s ("drop on demand").

Due to the complexity of the stent structure and the fact that the stents must rotate during the coating process, an algorithm was designed. The coating pattern defined by the algorithm where according to it, the dispenser moves longitudinally and vertically on the stent forming a perpendicular rectangular shape from one side of the stent to the other jetting one droplet/50 $\mu$ m (Fig. 2a). As shown in Fig. 1a he stents are place on a rotating holder where at the end of each coating pattern the holder rotates at 45<sup>o</sup> to coat the next side. The operation process is controlled by a stroboscope, which control if the dispenser jets according to the standards (Fig. 1b).

## **Scanning Electron Microscopy**

The quality of the coating was investigated using Scanning Electron Microscopy. The samples were attached to aluminum stubs with double-sided adhesive carbon tape, and examined using a scanning electron microscope (JEOL JSM 5310LV, SEM) in the low vacuum mode at 20 Pa. The working distance was between 35 and 45mm and the image captures using Oxford instrument ISIS 300 Autobeam software.

## **Atomic Force Microscopy (AFM)**

AFM analysis was performed on tapping mode using an easyscan AFM (Nanosurf, Lielestal, Switzerland). Tap 190Al-G cantilevers were used (budgetsensor, Sofia, Bulgaria). The drive amplitude and the relative set point were chosen in a way that the intermittent force between the oscillated tip and the substrate would be minimum and the scan areas was 5 $\mu$ m. The analysis of the images was performed using SPIP software (Image Metrology, Hørsholm, Denmark).

## **Transition temperature microscopy (TTM)**

TTM was carried using a VESTA<sup>TM</sup> system equipped with an AN-200 ThermoLever probe both from Anasys Instruments (Santa Barbara, USA). This technique is an extension of localised thermal analysis (LTA) where probes similar to those used in atomic force microscopy (AFM) are employed to provide controlled heating to site-specific areas on a sample surface. The voltage was calibrated for temperature by carrying out LTA measurements on three standard polymeric samples with known melting points. The experiments were carried out from room temperature at a heating rate of 10 °C/s. For each sample, an area of 100 x 100  $\mu$ m<sup>2</sup> was analysed at a resolution of 2  $\mu$ m. Each sample was mounted on stainless steel magnetic pucks for analysis.

## **Cell vitality and proliferation assay**

This test was performed following the International and European standards (ISO 10993-5/EN 30993-5) with the human pulmonary microvascular endothelial cell line (HPMEC-ST1.6R).<sup>22</sup> The cells were cultured in endothelial cell growth medium MV (Promocell GmbH, Heidelberg, Germany) enriched with endothelial cell growth supplement (Promocell GmbH, Heidelberg, Germany), streptomycin (0.1 g/L) and penicillin (100 IU/mL), at 37°C in a CO<sub>2</sub> incubator (CB 150/APT line/Binder, LabExchange, Paris, France) with 5% CO<sub>2</sub>/ 95% atmosphere and 100% relative humidity. The proliferation and vitality of cells were evaluated as previously described. Briefly, 6000 cells were seeded on the sterilized CoCr or CoCr/PLA disks and incubated for 3 and 6 days, then cell numbers were counted with Coulter Z1 cell counter (Beckman Coulter, France) and the cell vitality was evaluated by fluorometric analysis (Twinkle LB970TM Berthold) of AlamarBlue<sup>®</sup> dye (Interchim). Results were expressed as percentage compared to the cell growth on tissue-culture polystyrenes surface (TCPS).

## **Immunofluorescence imaging of cell adhesion to disk samples**

The cytoskeletal organization of the HPMEC growing on disk samples at 48 hours after cell seeding have been visualized by fluorescent-labeling of F-actin. Briefly, the cells were seeded on CoCr disk samples with and without PLA coating. Two days later, cells were fixed in 2% paraformaldehyde for 30 minutes at room temperature, permeabilized in a PBS/Triton X-100 buffer (10 mM PBS, 0.2% Triton) for 15 minutes, and then blocked with 1% bovine serum albumin (BSA, Sigma) in PBS. Actin filaments, vinculin and nuclei were stained with fluorescein-labelled phalloidin (Sigma) and 4,6-diamidino-2-phenylindole (DAPI) in VECTASHIELD<sup>®</sup> mounting medium (VECTOR laboratories), respectively, according to the

manufacturer's protocol. The samples observed by confocal laser scanning microscopy (LSM710, Zeiss, Germany).

### **Stent implantation in rat model of in-stent stenosis**

Male Wistar rats (Janvier, Le Gesnest-Saint-Isles, France, n=5), weighing 350 to 400 g, were randomly separated into the following groups: a) negative control with a CoCr bare metal stent, b) positive control with a Cypher stent and c) tested groups with SMV/PLA and PCX/PLA stents). On the day of implantation,<sup>23</sup> the rats were anesthetized (ketamine 130 mg/kg and xylazine 14 mg/kg intraperitoneally) and the abdomen was opened by a sagittal incision (NIH Guide for Care and Use of Laboratory Animals). Under microscopic view, the abdominal aorta was separated from the vena cava, and small side branches from the aorta were ligated. An arteriotomy was made in the proximal part of the 2.5 cm-long isolated infrarenal aortic segment. Thereafter, a premounted bare-metal stent (BMS), 2.5 × 14 mm, or PLA coated stents, 2.5 × 14 mm, was deployed at its nominal pressure (8 atm).

### **Histomorphological analysis**

As previously described,<sup>24</sup> stented arteries were fixed in 4% paraformaldehyde phosphate-buffered solution, dehydrated, and embedded in methylmethacrylate polymer (Technovit 9100 new, Heraeus, Germany). Sections 60µm thick were cut along the entire embedded stented vessels, stained with Mayer hematoxylin and eosin and examined under light microscopy (Leika DMIL, Germany) with magnification of x5. Images were digitized and recorded with the use of a video camera (AxioCam ERc 5s, Carl Zeiss Microscopy, Germany). For each stented vessel, 15 sections along the entire length were randomly chosen for the morphometric analysis, performed with a computerized digital microscopic planimetry algorithm by an independent observer blinded to drug regimen. Cross-sectional

areas of media, intima, and lumen were measured. Neointimal thickening was expressed as the ratio of the neointima area to the media area (n/m).

### **Cytokines array with PLA**

At 7 days after stent implantation, the animals were anesthetized and heparinized. The stented rat aortas were carefully removed, as the inflammatory response is an early event after stent deployment. Stented aortic segments were placed in lysis buffer, and the stent was carefully removed under optical control. Cytokines array was performed according to the manufacturer's instruction (Proteome Profiler Rat Cytokine Array, R&D Systems, France). Equal amount of proteins (300 µg) were incubated with a detection antibody cocktail for 1 hour at room temperature. Then each sample/antibodies mixture was incubated overnight with a nitrocellulose membrane with spotted antibodies at 6°C. Bound antibodies were visualized by ECL and quantified by densitometric analysis.

### **Drug loading**

The drug loading for each coated stent was determined by placing the stent in an HPLC vial and the addition of 1ml acetonitrile (ACN). The samples were sonicated for 10mins (Sonicwave, Cardiff, U.K.) 20min and subsequently the drug amounts were estimated by HPLC analysis. The yield of the stent was determined by jetting equal amount of droplets on round stainless steel disks for each drug-polymer solution, followed by the addition of 1ml acetonitrile and subsequent HPLC analysis. The following equation was used to calculate the final coating yield:

$$Yield (Y) = \frac{Drug_{disk} - Drug_{stent}}{Drug_{disk}} \times 100 \quad (1)$$

## **Dissolution Studies**

The drug-loaded stents (SMV, PCX) were immersed in test tubes containing 2 ml sterilized PBS (pH 7.4). The tubes were then incubated in a water-bath shaker at 37°C at 120 rpm. The incubated PBS in each tube was collected and replaced with fresh buffer system everyday.

## **HPLC analysis**

Agilent technologies 1200 series with a quaternary pump, an autosampler and a detector set at 250nm for simvastatin and 227nm for paclitaxel respectively. The column was an Agilent Zorbax Eclipse XDB-C8 (4.6 mm × 150 mm, 5 μm particle size) heated at 40°C with a flow rate at 1ml/min injection volumes of 20μl. The Chemstation software calculated the peak area of each standard solution and sample automatically. In the case of simvastatin the mobile phases consisted of water:formic acid (0.1%) (Phase A) and acetonitrile:formic acid (0.1%) (phase B) (A:B = 30:70). For paclitaxel, analysis the mobile phase consisted of water:acetonitrile (60:40).

## **2. Results & Discussion**

### **Ink jetting of biocompatible polymers**

The selected drug - polymer ratios of the coating formulations were 1:3 (w/w) similar to the marketed DES, which subsequently were dissolved, in organic solvents. The jetting process optimized by assessing various solvents in order to achieve uniform and reproducible coatings. For these reason solvents with high boiling point such as butanone and acetonitrile or mixtures with DCM were initially tested. However, this resulted to non-uniform coating with uncoated areas on the strut surface due to the slow evaporation of the deposited material, which led in droplet accumulation. The jetting optimization revealed that DCM (Class III) was the suitable organic solvent to produce uniform, accurate and reproducible coating. Due

to the small droplet particle size and the solvent volatility DCM evaporates rapidly (40°C boiling point) forming the desired drug/polymer layers. However, continuous ink jetting can cause a gradual accumulation of polymer at the edge of the nozzle, therefore, Nanoplotter was programmed to wash the tip periodically with solvent and water solutions. As shown in Fig. 1b the particle size of the droplets is observed with a stroboscope, which controls the coating process by periodically inspecting the droplet formation from the dispenser. The stroboscope can provide qualitative analysis of the droplets generated during the dispensing process and provide an approximate estimation of the droplet size.

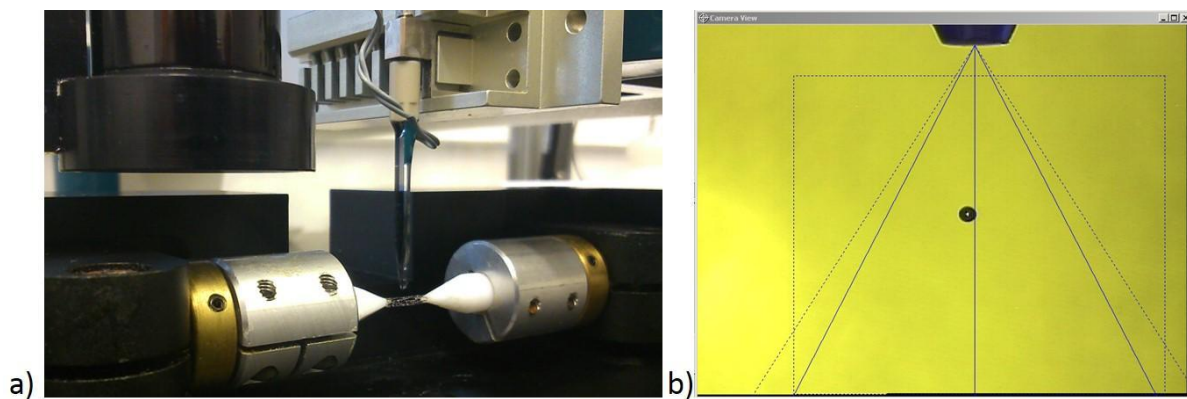


**Figure 1:** a) Image of the piezoelectric dispenser and stent holder of the Nanoplotter device during the coating process and, b) stroboscope image of the droplet as ejected from the dispenser

The efficiency of jetting of coating solutions onto the stent strut depends considerably on the tip size, the applied voltage<sup>14</sup> on the piezoelectric material and the pulse duration (ms). Our evaluation showed that tips with 300 pl aqueous droplet volume are suitable for stent coating. Tips generating smaller volumes (100 pl) resulted in clogging of the nozzle while larger volumes ejected larger droplets, which caused bridge formation between the strut curvatures. It has been proved that the fluid volume ejected from the dispenser and as a consequence the droplet size is a linear function of the voltage.<sup>25</sup> For a given coating solution the increase of the applied voltage will increase the droplet diameter whereas increase of pulse duration will result to a more complicated and periodic behaviour.<sup>26</sup> It is also worth mentioning that high

voltages can cause air bubble formation inside the tip when low surface tension liquids are used as in the case of organic solvents. The jetting optimization (data not shown) for the SMV/PLA and PCX/PLA solutions showed that the applied voltage and pulse vary according to the complexity of the stent design whereas combined jetting patterns should be employed. Fig 2 illustrates typical coating patterns for ink jetting of a stent surface.

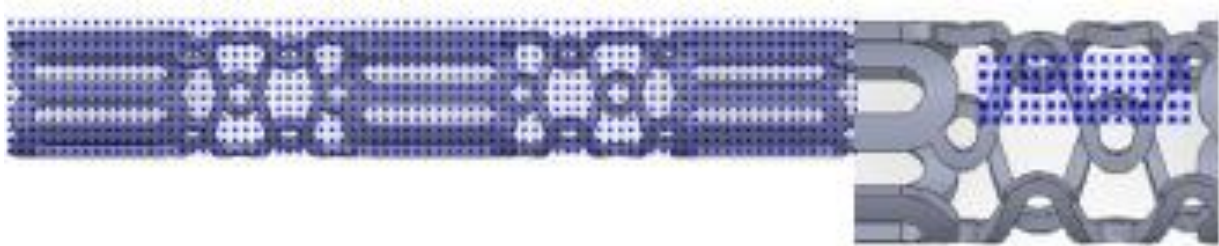


**Figure 2:** coating patterns of Cypher® stents a) for large areas of the stent struts, b) for smaller areas with thin struts

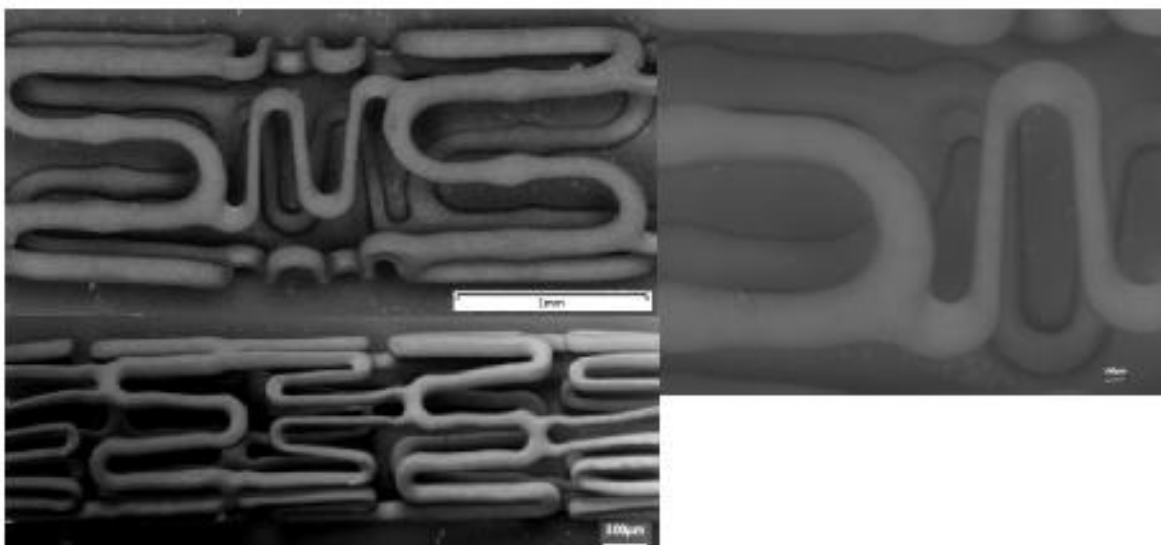


**Figure 3:** SEM images of a) Cypher® stent b) Presillion® stent and c) higher magnification on the surface of Cypher® stent

The Cypher® stent possess more complex design than Presillion®, with six circumferential cells and ultra-thin links connecting the cells. These curvy ultra-thin stent links were more difficult to coat as the droplets tended to accumulate at the edges. Therefore, the links were targeted separately after the first coating (Fig. 2b). The applied voltage and pulse duration for

the wider strut surfaces were 100V and 60 $\mu$ sec respectively (Fig 2a) while for the thin parts 60V and 60 $\mu$ sec (Fig 2b).

The voltage reduction facilitated the formation of smaller droplet size without any splashing and thus reduced material losses. The quality of stent coating is very important as affects the release profile of the therapeutic agent while smooth surface coatings can significantly decrease the injury of blood vessel. Tepe *et al.* evaluated different peripheral stents and found that smoothing the surface results to a clear decrease of their thrombogenicity.<sup>27</sup> Furthermore, uniform coating without cracks and bridges is required for a homogenous release across the total stent strut. The SEM images in Fig. 3 showed smooth and uniform drug/polymer layers for the obtained coatings irrespectively of the stent design and without any bridges forming between the struts. The coating efficiency of ink jetting was assessed in terms of the obtained yields. As show in Table 1, ink jetting of the Presillion<sup>®</sup> stent provided far better yield compared to Cypher<sup>®</sup>. This is probably due to the less complex design of Presillion<sup>®</sup> although both stents have a closed-cell design. Also, the reproducibility for Cypher<sup>®</sup> is  $\pm 6.49\%$  and  $\pm 4.05\%$  for Presillion<sup>®</sup> which is acceptable from the industry.

### **Atomic Force Microscopy (AFM)**

AFM images of coated stent with SMV/PLA and PCX/PLA are shown in Fig. 4. In both mixtures, the coating is homogenous without any phase separation. Roughness analysis showed that the roughness of PCX/PLA and SMV/PLA is 53.5nm and 85nm respectively indicating that the coating is almost flat. More importantly similar studies of AFM and confocal Raman microscopy showed that the estimated roughness of the marketed Cypher<sup>®</sup> stents is approximately 2 $\mu$ m rendering the stents produced by inkjet printing more advantageous.<sup>28</sup> It is worth mentioning that the bright areas in phase image of PCX/RES have been created due to the stronger interaction forces between the AFM tip and the surface when

the tip enters inside the pores. These pores in both topographic images is a common are usually observed in solvent casting polymer layers or stent coatings and are formed due to solvent evaporation.

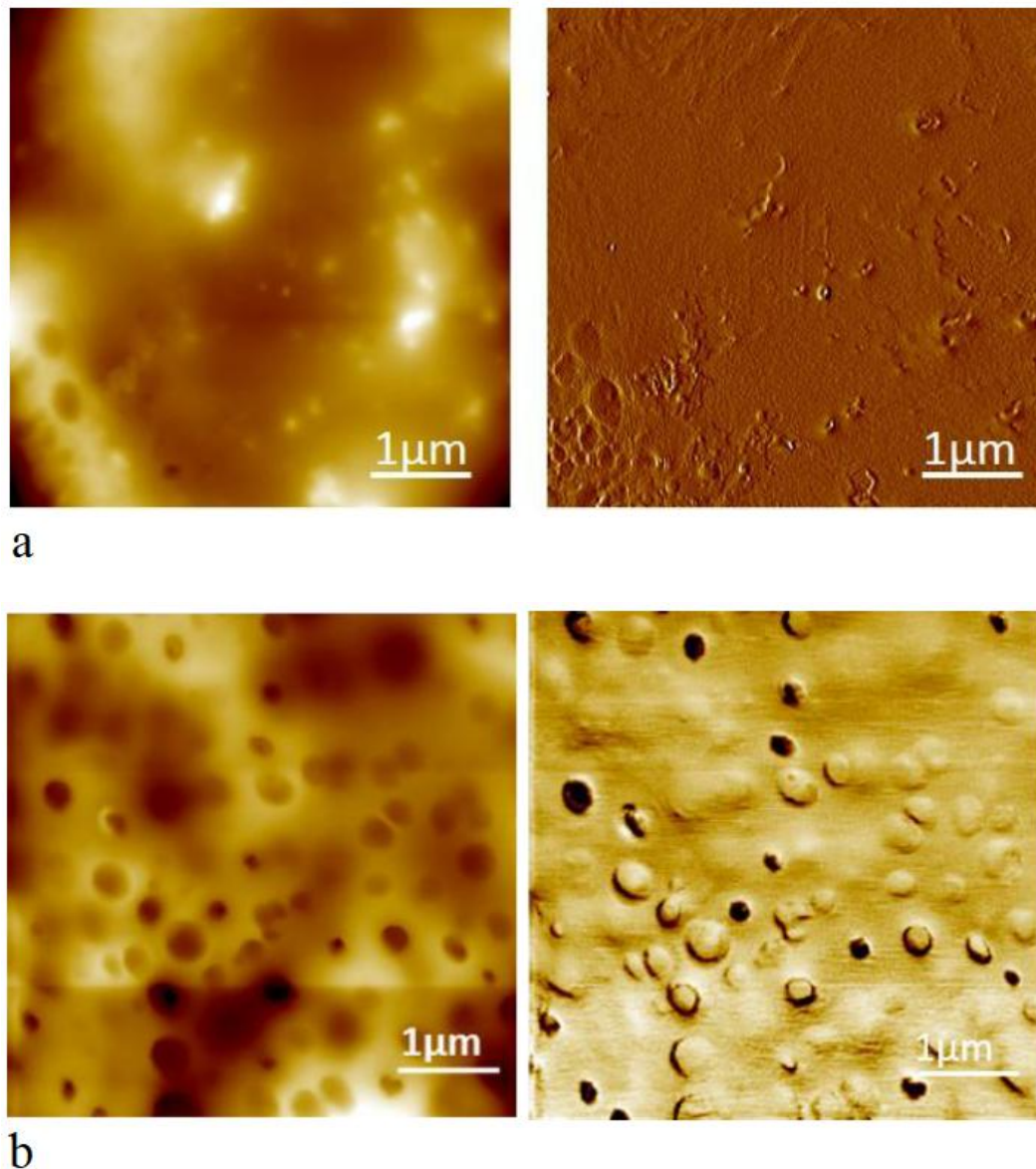
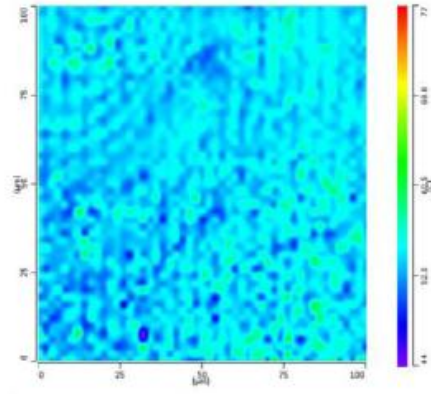
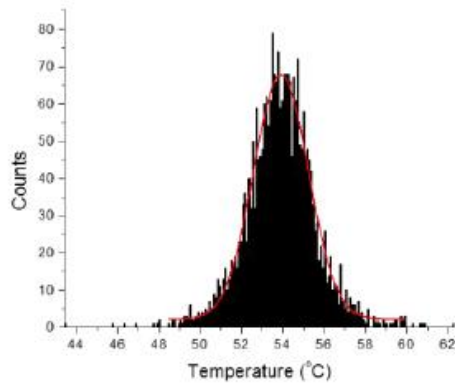


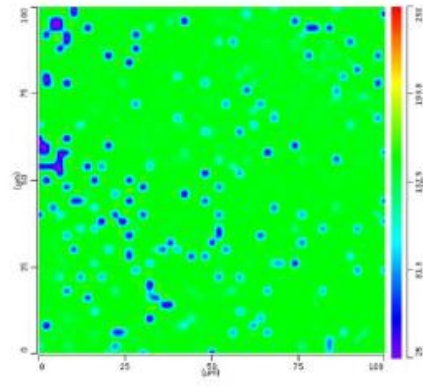
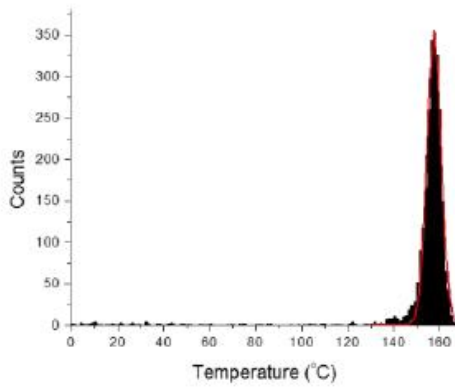
**Figure 4:** Topographic (left) and Phase (right) AFM images of a) PCX/PLA and b) SMV/PLA

### TTM Analysis

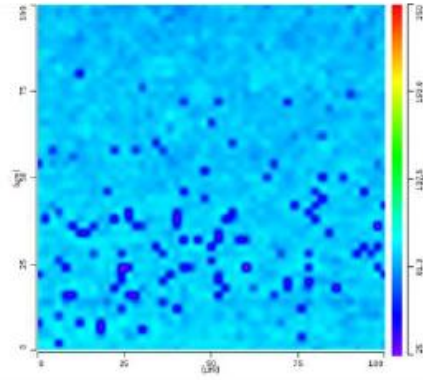
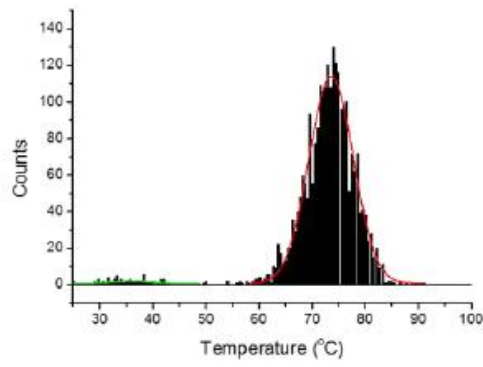
Fig. 5 shows a typical TTM analysis, which involves placement of the probe at a chosen location and the application of a scanning voltage profile whilst simultaneously monitoring the probe deflection.



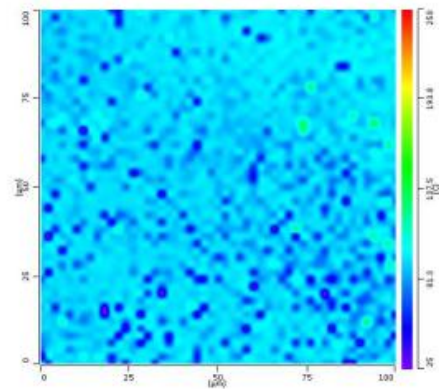
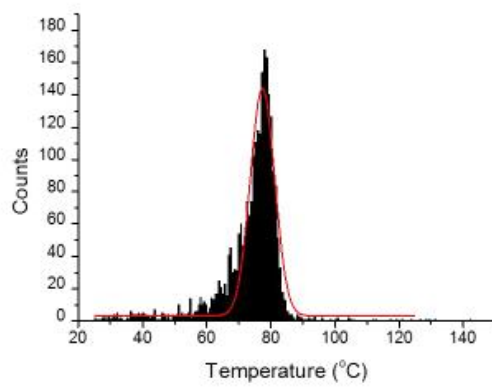
a



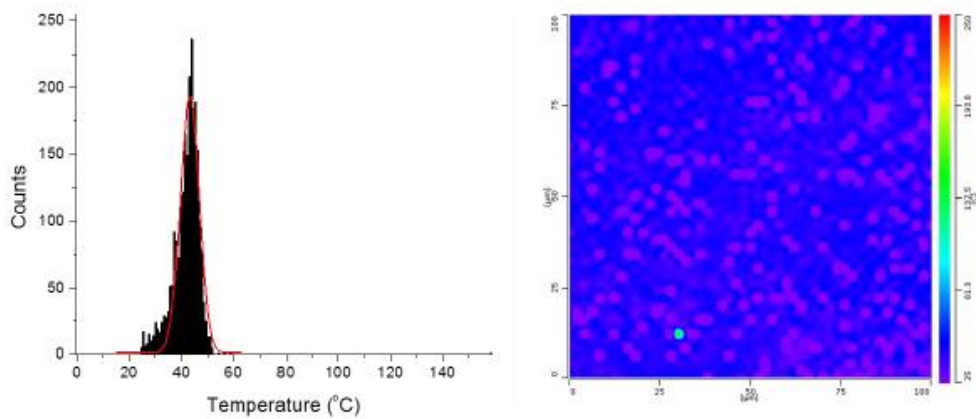
b



c



d



e

**Figure 5:** TTM maps and histograms (right) of a) pure sprayed PLA, b) pure sprayed PCX, c) pure sprayed SMV d) PCX/PLA mixture and e) SMV/PLA mixture

Due to thermal expansion of the material being heated, the probe deflects upwards until a thermal event occurs, such as melting, where probe penetration is observed as downwards deflection due to the material softening. As expected the initial analysis of plain PLA coating layers, showed a mean value of the glass transition<sup>29</sup> at 53.9°C while the Gaussian distribution in Fig. 5a indicates a single phase. As shown in fig. 5b for coated bulk APIs the TTM analysis revealed a gaussian distribution with a mean value of 148°C for PCX which is close to the experimental value reported in literature (153°C).<sup>30</sup> However, in the case of SIMV a bimodal distribution can be observed where the first broad peak lies close to the Tg of SIMV (35°C)<sup>31</sup> and the second stronger peak at 74°C, which corresponds to crystalline drug (Fig. 5c).

In the case of PXL/PLA coated layers TTM analysis showed a unimodal distribution with a single Tg at 78°C indicating the homogeneity of the binary mixture (Fig. 5d). The observed Tg lies between the PXL and PLA Tgs suggesting that PXL is molecularly dispersed in the polymer matrix. Similar results with a single Tg at 44°C were observed for the SMV/PLA coatings with SMV being molecularly dispersed in the polymer matrix (Fig. 5e). The results

are in agreement with the AFM observations, which showed that there is no phase separation between the components. It is worth mentioning that the distribution is negatively skewed in the case of PCX/PLA coatings due to the higher concentration of polymer, which shifts the Tg of the mixture to lower values.

### Cell vitality and proliferation assay

In order to investigate the cytocompatibility of the stent coating polymer, cell vitality and proliferation assay were implemented. Several studies have been reported to investigate the proliferation, morphology and attachment of different types of cells on various drug delivery systems or medical implants where all confirmed the biocompatibility of PLA.<sup>32, 33</sup>

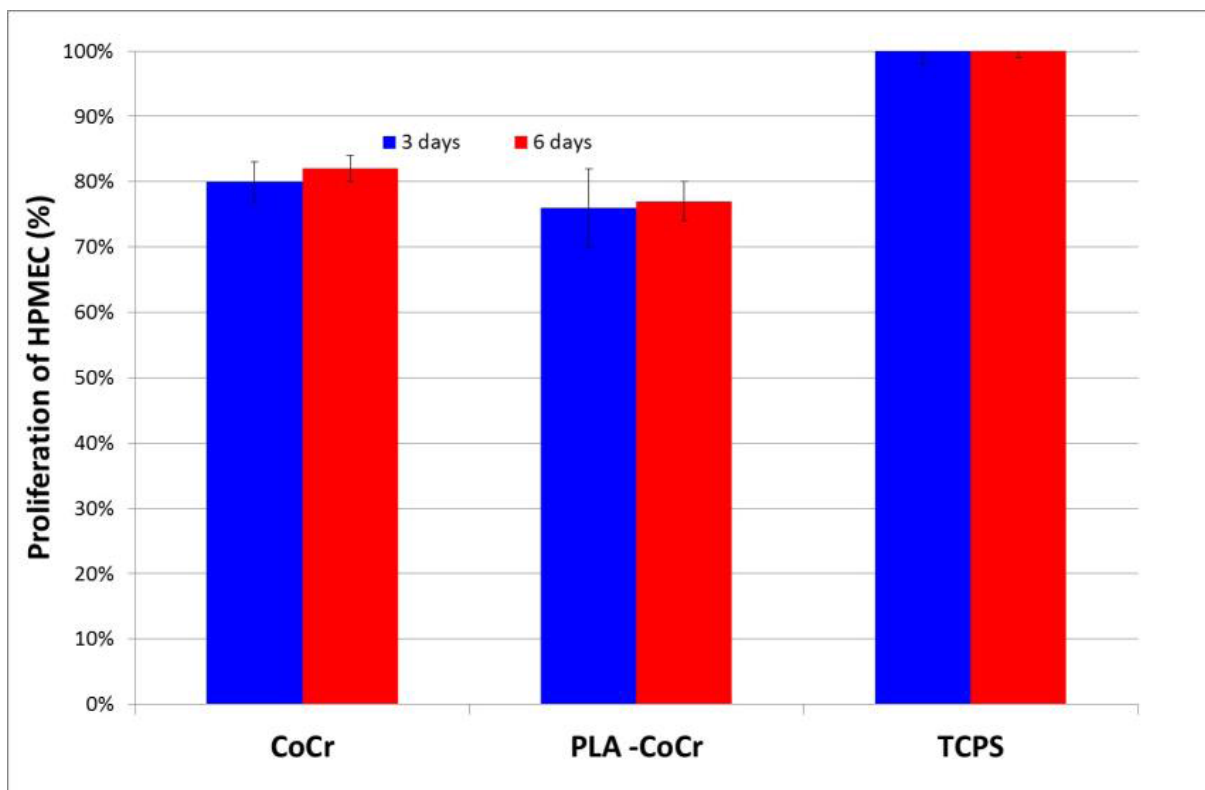


**Figure 6:** Graphs of HPMEC vitality and proliferation on CoCr, Resomer-Cocr and TCPS substrates

Yet, the use of organic solvent to dissolve the compounds could have a detrimental effect regarding coating's biocompatibility due to the presence of any residues. The results showed

a significant difference of cell proliferation or vitality between CoCr disk groups and TCPS (Fig. 6). Although the vitality rate and proliferation level were slightly lower on disk samples (~80%) than that on TCPS (100%), there is no significant difference between CoCr and CoCr/PLA samples. Thus, it was concluded that PLA coatings did not decrease the vitality or proliferation of cells, and confirmed the *in vitro* biocompatibility of the polymeric carrier. In addition, the results provide strong evidence that DCM has been removed and there are no any solvent residues in the coated layers, which would result in reduced cell viability.

### **Immunofluorescence imaging and cell adhesion**

Concerning the cell adhesion at 48 hours after cell seeding, cells were well spreading over non-coated CoCr surface with a normal cytoskeleton. As shown in Fig. 7a the cells appear to have long green bundles of stress fibres composed of actin filaments. In Fig. 7b the cells, on the PLA coated CoCr surface, are wide-spreading with well-defined actin filaments showing a similar morphology to those of the non-coated CoCr disks. The organization of the cytoskeleton on PLA coated CoCr disks confirmed the excellent cell-substrate adhesion.

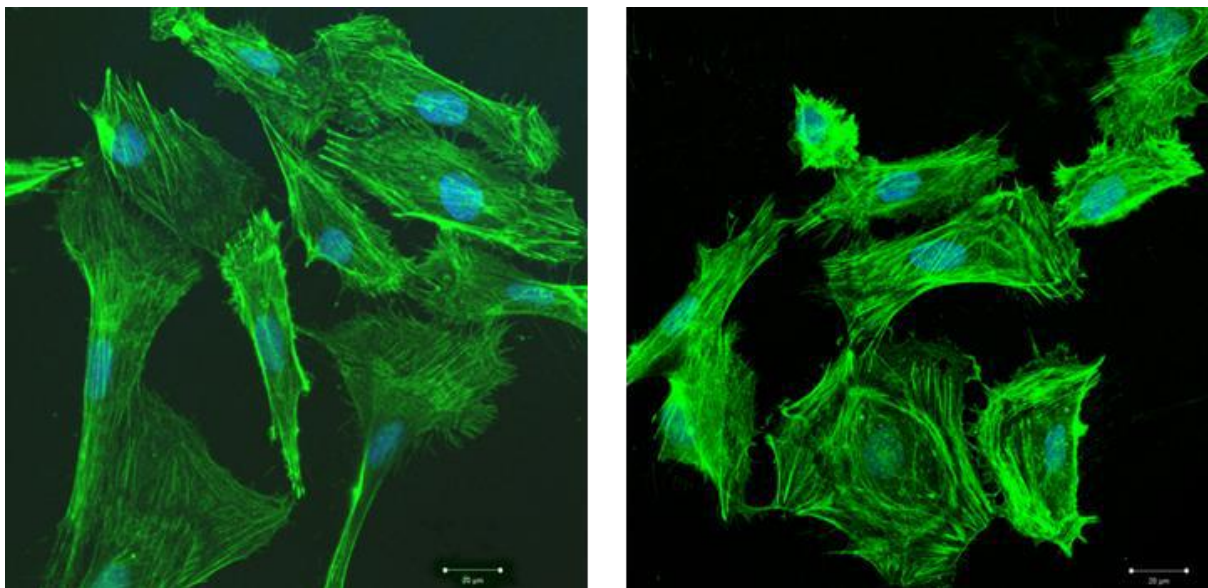


**Figure 7:** Fluorescence microscopy images on HPMEC on CoCr (left) and on CoCr/Resomer (right) samples

## Cytokines array with PLA

Further studies investigated the levels of several cytokines and inflammatory adhesion molecules in stented aortic segments 7 days after stent deployment. The implanted stents were coated only with the PLA polymer without containing any anti-proliferative agent, as the aim was only to evaluate the *in vivo* toxicity of the PLA coating. The protein array revealed no significant variation of several immunogenic and chemo-attractive cytokines expression, such as interleukin 6 and tumour necrosis factor- $\alpha$ , as well as adhesive molecules expression such as intercellular adhesion molecule. Fig. 8 illustrates the recorded levels of the investigated molecules between the implanted PLA coated stents and the controls (n = 3). The results obtained from the *in vivo* implantation demonstrated that the PLA coatings did not increase the inflammatory response after stent implantation, comparing with bare metal stent. Nevertheless, further studies are required to evaluate the inflammatory response of the drug coated stents.

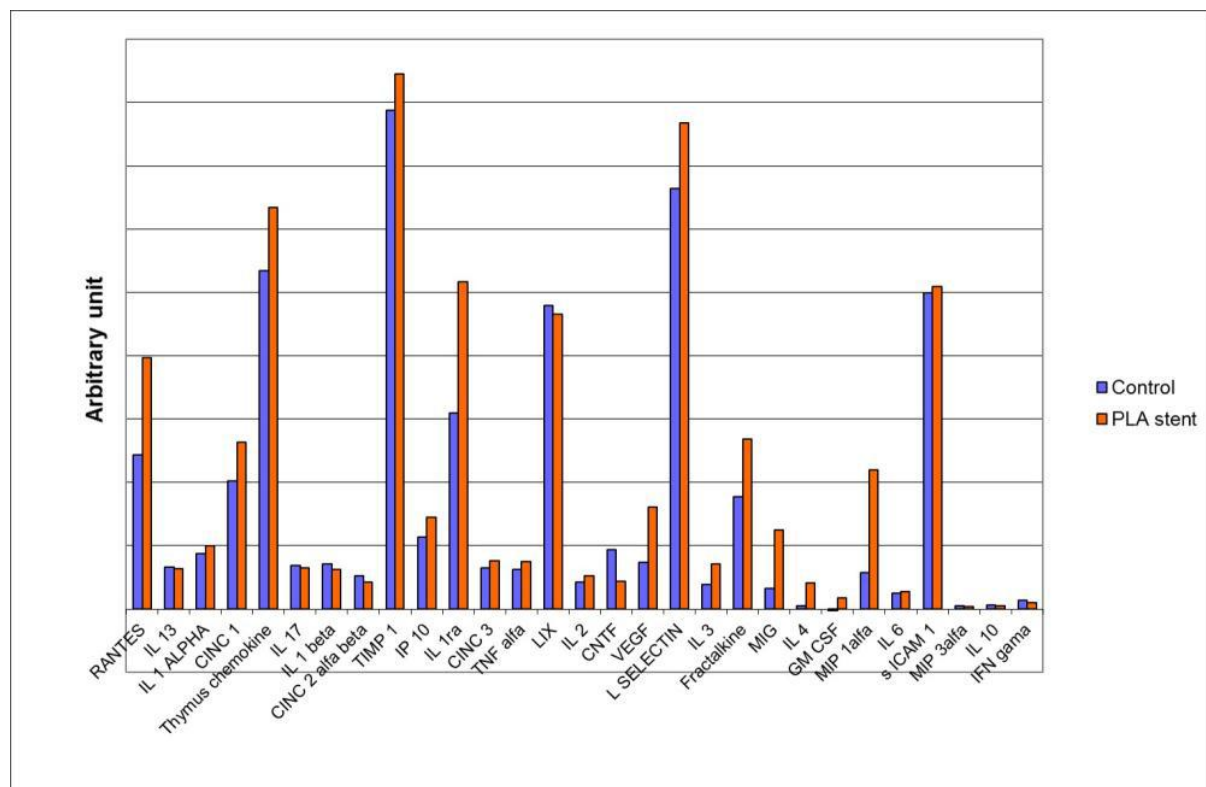


**Figure 8:** Comparison Cytokines for PLA and control coated CoCr disks.

## Histomorphological analysis

As shown in Fig. 9 the DES developed by inkjet printing implanted in Male Wistar rats for comparison with BMS (negative control) and Cypher stents (positive control). Fig. 10 shows the histomorphological analysis of the stented aortic sections for the implanted stents

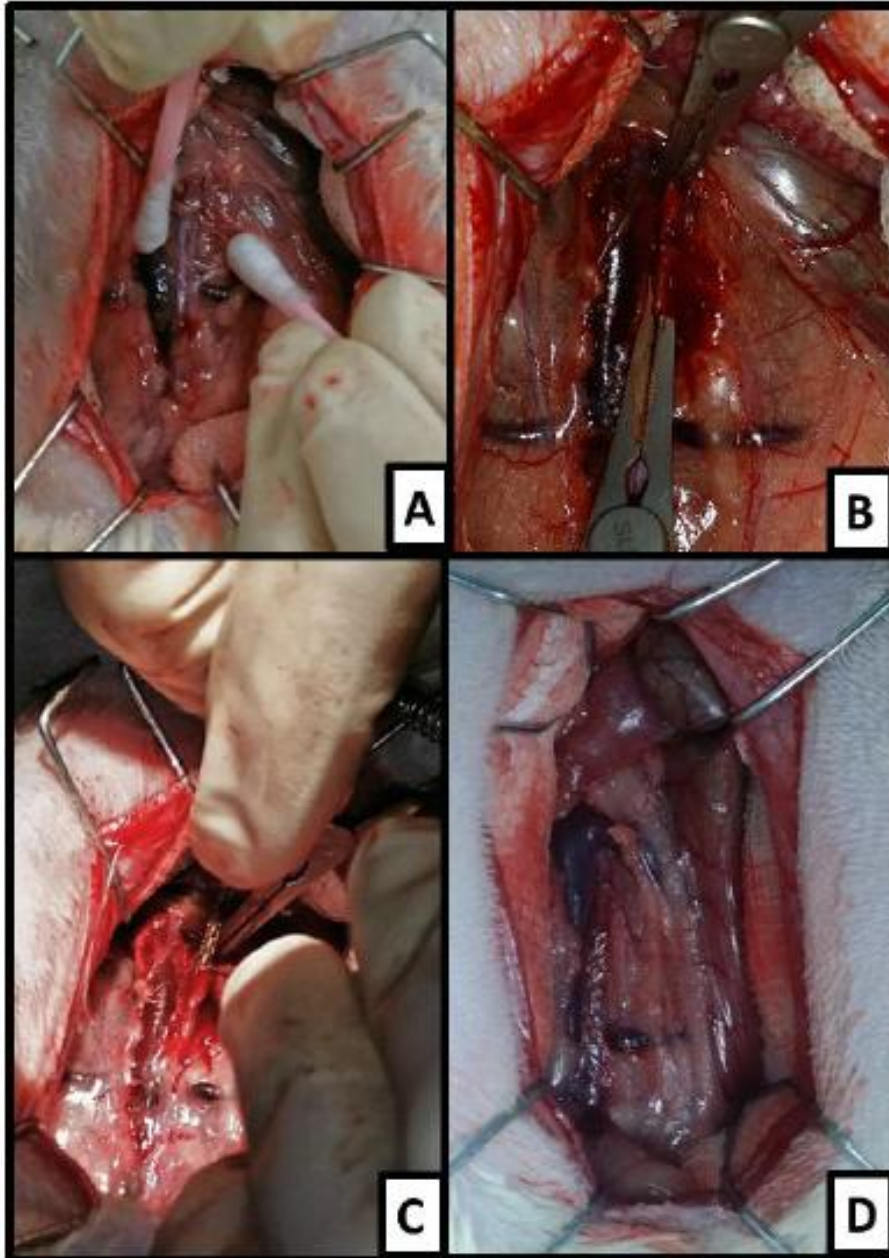


**Figure 9:** Stent implantation in Male Wistar rats: a) infra-renal aorta exposition, b) aortic cross-clamping and transverse aortotomy, c) stent insertion, d) infrarenal stenting and closure of the aortotomy.

As it can be seen from Fig. 11 the analysis revealed the same reduction in neointima formation between the plain PLA coated stent compared to the negative control BMS and confirmed the *in vitro* cell proliferation results.

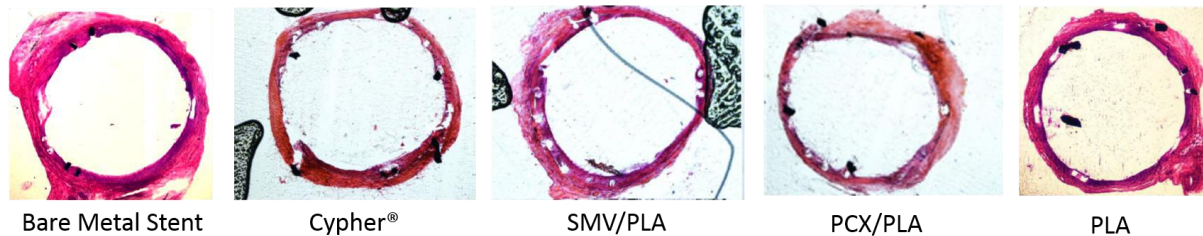


**Figure 10:** Images of the ISR for the BMS, Positive Control stent, SMV and PCX coated stent.

The results also demonstrate lower ISR of the PCX/PLA (n/m 0.67) compared to BMS (n/m 0.73), which demonstrates the clinical effect of PXL from inkjet printing stents. In addition PXC/PLA stents show a slightly higher ISR values compared to the marketed Cypher stents (positive control). However this is not uncommon as<sup>34</sup> PXL demonstrated significant reduction in late lumen loss, diameter stenosis and neointimal hyperplasia but not a dramatic reduction in the incidence ISR compared to sirolimus.

As shown in Fig. 11 an unexpected ISR (1.02) reduction was observed for the SMV/PLA stents compared to the negative control. SMV demonstrated encouraging results in the past by reducing neointimal formation in the human saphenous vein, inhibiting VSMC proliferation and migration.<sup>35, 36</sup> However there are cases where SMV demonstrated insufficient performance and did not facilitate any ISR reduction after stent implantation.<sup>37, 38</sup>

In this case, further investigation is required and perhaps an increase of the SMV/PLA ratio could provide better ISR results. Nevertheless, the obtained experimental findings showed that inkjet printing is a robust technology, which can be employed for the development of DES.

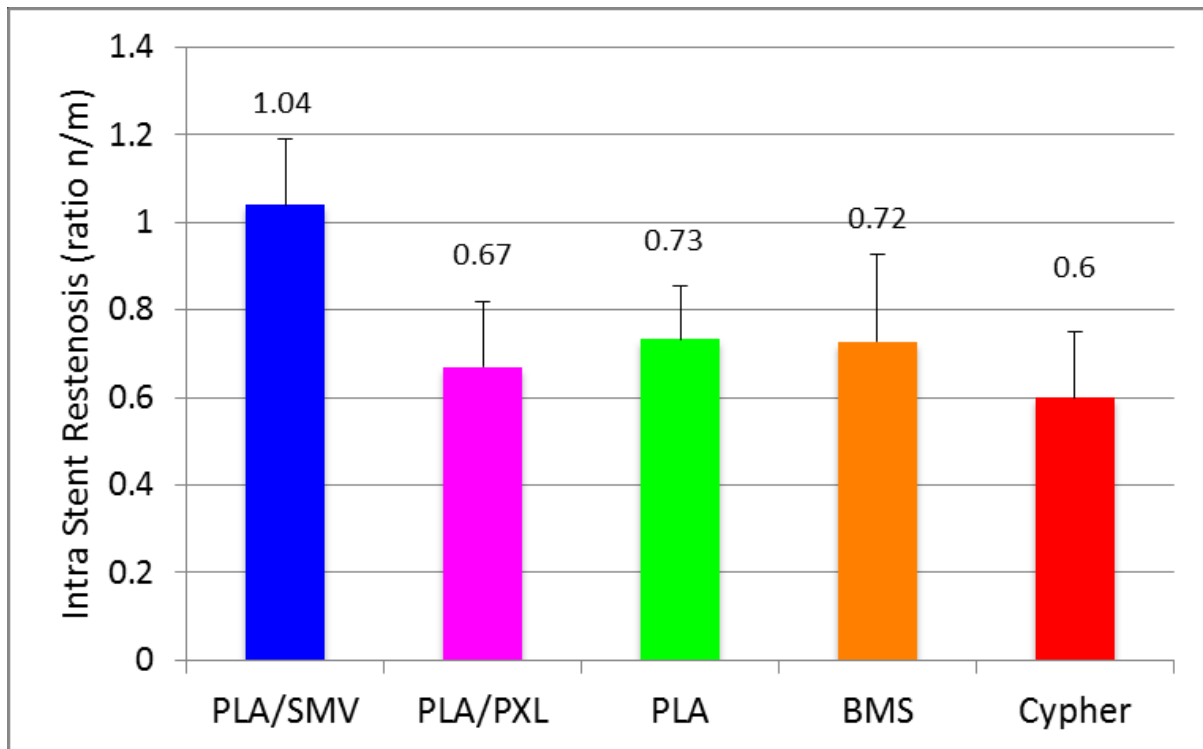


**Figure 11:** Quantification of the ISR for BMS, Positive Control stent, SMV and PCX coated stent

## Drug Release

The in vitro drug release rates from the stent strut are important for the development of DES and can be controlled by adjusting the drug/polymer ratio. PLA has been extensively used to control the drug release mainly in the form of nanoparticles but it has also been implemented in various biomedical applications.<sup>39</sup> The cumulative drug release profiles of SMV and PCX are represented in Figure 11.

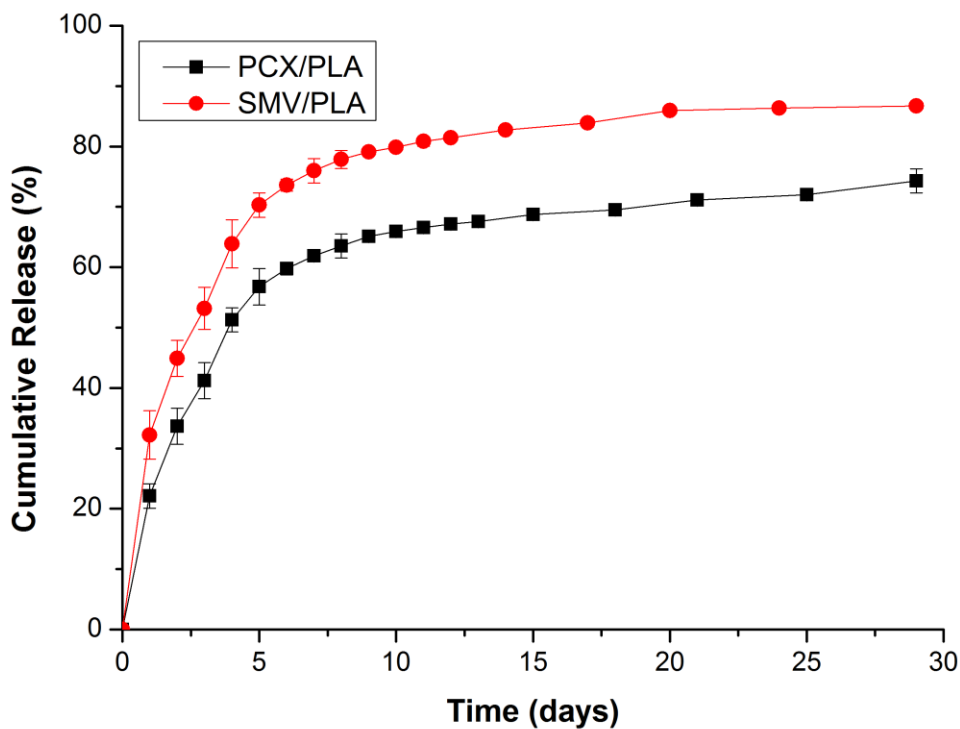


**Figure 12:** Dissolution profiles of SMV/PLA (1:3 wt/wt) and PCX/PLA (1:3 wt/wt) coated stents with 100µg of drug substances (n=3)

As it can be seen both drugs exhibit burst release for the first 5 days, followed by slower release rates. This is not uncommon in DES and it has been observed in similar studies.<sup>35, 40</sup>

As it can be seen the burst release is of the magnitude of 22% and 35 % for PCX and SMV respectively. At the end of the study period, 80% of SMV and 75% of PXC were released.

The increased burst release of SMV compared to PCX is associated to the phase separation of the drug from the polymer. In contrast PCX interacts with PLA forming a homogenous mixture, as confirmed by AFM and TTM, which in turn delays the release rates. After the initial burst release both drugs followed a first order release for another 25 days. However, we anticipate that the *in vivo* performance of PXC and SMV release rates will substantially differ from those shown in Fig. 11. Nevertheless, the drug release studies demonstrated a sustained release pattern for both types of DES. An important aspect of ink jetting is that by adjusting the drug/polymer ratio in the coating solution or by using different polymer grades

the stent release profiles can be and the applied drug substance amounts tuned accordingly to the patient needs.

## **Conclusion**

In this study, inkjet-printing technology has been used successfully to apply uniform and reproducible PCL/PLA and SMV/PLA coatings. The drug/polymer compositions did not have any influence on the coating uniformity while the obtained yields were found to be dependant on the stent design. The *in vitro* evaluation showed excellent polymer cell proliferation and cell adhesion. The stent implantation in animal models demonstrated the absence of inflammatory response and the reduction of ISR similar to marketed bare metal and drug eluting stents. Overall, inkjet-printing technology can be effectively used for the optimization of robust drug eluting stents and the application of wide range drug/polymer uniform layers with controlled drug release patterns.

## **Acknowledgements**

The authors would like to thank Dr Adrien Hertault and Mr. Mickael Maton for their precious assistance in *in vivo* experimental study. We also thank the Plate-forme Ressources Expérimentales, D.H.U.R.E, Faculté de Médecine, University of Lille 2 for their supporting on animal studies.

This work was fully supported by the cross – border INTERREG IV A “2 Mers Seas Zeeën” cooperation program 2007 - 2013.

## **Declaration**

The authors report no conflict of interest

## References

1. Garg, S.; Serruys, P. W., Coronary Stents: Looking Forward. *Journal of the American College of Cardiology* **2010**, 56, (10, Supplement), S43-S78.
2. Kukreja, N.; Onuma, Y.; Daemen, J.; Serruys, P. W., The future of drug-eluting stents. *Pharmacological Research* **2008**, 57, (3), 171-180.
3. Lemos, P. A.; Moulin, B.; Perin, M. A.; Oliveira, L. A. R. R.; Arruda, J. A.; Lima, V. C.; Lima, A. A. G.; Caramori, P. R. A.; Medeiros, C. R.; Barbosa, M. R.; Brito, F. S.; Ribeiro, E. E.; Martinez, E. E., Randomized evaluation of two drug-eluting stents with identical metallic platform and biodegradable polymer but different agents (paclitaxel or sirolimus) compared against bare stents: 1-Year results of the PAINT trial. *Catheterization and Cardiovascular Interventions* **2009**, 74, (5), 665-673.
4. Stettler, C.; Wandel, S.; Allemann, S.; Kastrati, A.; Morice, M. C.; Schomig, A.; Pfisterer, M. E.; Stone, G. W.; Leon, M. B.; de Lezo, J. S.; Goy, J. J.; Park, S. J.; Sabate, M.; Suttorp, M. J.; Kelbaek, H.; Spaulding, C.; Menichelli, M.; Vermeersch, P.; Dirksen, M. T.; Cervinka, P.; Petronio, A. S.; Nordmann, A. J.; Diem, P.; Meier, B.; Zwahlen, M.; Reichenbach, S.; Trelle, S.; Windecker, S.; Juni, P., Outcomes associated with drug-eluting and bare-metal stents: a collaborative network meta-analysis. *Lancet* **2007**, 370, (9591), 937-48.
5. Wilson, G. J.; Nakazawa, G.; Schwartz, R. S.; Huibregtse, B.; Poff, B.; Herbst, T. J.; Baim, D. S.; Virmani, R., Comparison of Inflammatory Response After Implantation of Sirolimus- and Paclitaxel-Eluting Stents in Porcine Coronary Arteries. *Circulation* **2009**, 120, (2), 141-149.
6. Finn, A. V.; Kolodgie, F. D.; Harnek, J.; Guerrero, L. J.; Acampado, E.; Tefera, K.; Skoriya, K.; Weber, D. K.; Gold, H. K.; Virmani, R., Differential response of delayed healing and persistent inflammation at sites of overlapping sirolimus- or paclitaxel-eluting stents. *Circulation* **2005**, 112, (2), 270-8.
7. Finn, A. V.; Nakazawa, G.; Joner, M.; Kolodgie, F. D.; Mont, E. K.; Gold, H. K.; Virmani, R., Vascular responses to drug eluting stents: importance of delayed healing. *Arteriosclerosis, thrombosis, and vascular biology* **2007**, 27, (7), 1500-10.
8. Joner, M.; Nakazawa, G.; Finn, A. V.; Quee, S. C.; Coleman, L.; Acampado, E.; Wilson, P. S.; Skoriya, K.; Cheng, Q.; Xu, X.; Gold, H. K.; Kolodgie, F. D.; Virmani, R., Endothelial cell recovery between comparator polymer-based drug-eluting stents. *J Am Coll Cardiol* **2008**, 52, (5), 333-42.
9. Kim, T. G.; Lee, H.; Jang, Y.; Park, T. G., Controlled release of paclitaxel from heparinized metal stent fabricated by layer-by-layer assembly of polylysine and hyaluronic acid-g-poly(lactic-co-glycolic acid) micelles encapsulating paclitaxel. *Biomacromolecules* **2009**, 10, (6), 1532-9.
10. Hanefeld, P.; Westedt, U.; Wombacher, R.; Kissel, T.; Schaper, A.; Wendorff, J. H.; Greiner, A., Coating of Poly(p-xylylene) by PLA-PEO-PLA Triblock Copolymers with Excellent Polymer-Polymer Adhesion for Stent Applications. *Biomacromolecules* **2006**, 7, (7), 2086-2090.
11. San Juan, A.; Bala, M.; Hlawaty, H.; Portes, P.; Vranckx, R.; Feldman, L. J.; Letourneur, D., Development of a Functionalized Polymer for Stent Coating in the Arterial Delivery of Small Interfering RNA. *Biomacromolecules* **2009**, 10, (11), 3074-3080.
12. Meyers, S. R.; Kenan, D. J.; Khoo, X.; Grinstaff, M. W., Bioactive Stent Surface Coating That Promotes Endothelialization while Preventing Platelet Adhesion. *Biomacromolecules* **2011**, 12, (3), 533-539.

13. Saurer, E. M.; Jewell, C. M.; Roenneburg, D. A.; Bechler, S. L.; Torrealba, J. R.; Hacker, T. A.; Lynn, D. M., Polyelectrolyte Multilayers Promote Stent-Mediated Delivery of DNA to Vascular Tissue. *Biomacromolecules* **2013**, 14, (5), 1696-1704.
14. Scandinavian Simvastatin Survival Study, G., Randomised trial of cholesterol lowering in 4444 patients with coronary heart disease: the Scandinavian Simvastatin Survival Study (4S). *The Lancet* **1994**, 344, (8934), 1383-1389.
15. Indolfi, C.; Cioppa, A.; Stabile, E.; Lorenzo, E. D.; Esposito, G.; Pisani, A.; Leccia, A.; Cavuto, L.; Stingone, A. M.; Chieffo, A.; Capozzolo, C.; Chiariello, M., Effects of hydroxymethylglutaryl coenzyme A reductase inhibitor simvastatin on smooth muscle cell proliferation in vitro and neointimal formation in vivo after vascular injury. *Journal of the American College of Cardiology* **2000**, 35, (1), 214-221.
16. McDermott, M.; Chatterjee, S.; Hu, X.; Ash-Shakoor, A.; Avery, R.; Belyaeva, A.; Cruz, C.; Hughes, M.; Leadbetter, J.; Merkle, C.; Moot, T.; Parvinian, S.; Patwardhan, D.; Saylor, D.; Tang, N.; Zhang, T., Application of Quality by Design (QbD) Approach to Ultrasonic Atomization Spray Coating of Drug-Eluting Stents. *AAPS PharmSciTech* **2015**, 1-13.
17. Heldman, A. W.; Cheng, L.; Jenkins, G. M.; Heller, P. F.; Kim, D.-W.; Ware, M.; Nater, C.; Hruban, R. H.; Rezai, B.; Abella, B. S.; Bunge, K. E.; Kinsella, J. L.; Sollott, S. J.; Lakatta, E. G.; Brinker, J. A.; Hunter, W. L.; Froehlich, J. P., Paclitaxel Stent Coating Inhibits Neointimal Hyperplasia at 4 Weeks in a Porcine Model of Coronary Restenosis. *Circulation* **2001**, 103, (18), 2289-2295.
18. Scoutaris, N.; Alexander, M. R.; Gellert, P. R.; Roberts, C. J., Inkjet printing as a novel medicine formulation technique. *Journal of Controlled Release* **2011**, 156, (2), 179-185.
19. Buanz, A. M.; Saunders, M.; Basit, A.; Gaisford, S., Preparation of Personalized-dose Salbutamol Sulphate Oral Films with Thermal Ink-Jet Printing. *Pharm Res* **2011**, 28, (10), 2386-2392.
20. Uddin, M. J.; Scoutaris, N.; Klepetsanis, P.; Chowdry, B.; Prausnitz, M. R.; Douroumis, D., Inkjet printing of transdermal microneedles for the delivery of anticancer agents. *International Journal of Pharmaceutics*, (0).
21. Tarcha, P.; Verlee, D.; Hui, H.; Setesak, J.; Antohe, B.; Radulescu, D.; Wallace, D., The Application of Ink-Jet Technology for the Coating and Loading of Drug-Eluting Stents. *Annals of Biomedical Engineering* **2007**, 35, (10), 1791-1799.
22. Krump-Konvalinkova, V.; Bittinger, F.; Unger, R. E.; Peters, K.; Lehr, H. A.; Kirkpatrick, C. J., Generation of human pulmonary microvascular endothelial cell lines. *Laboratory investigation; a journal of technical methods and pathology* **2001**, 81, (12), 1717-27.
23. Lowe, H. C.; James, B.; Khachigian, L. M., A novel model of in-stent restenosis: rat aortic stenting. *Heart (British Cardiac Society)* **2005**, 91, (3), 393-5.
24. van Beusekom, H. M. M.; Whelan, D. M.; van de Plas, M.; van der Giessen, W. J., A practical and rapid method of histological processing for examination of coronary arteries containing metallic stents. *Cardiovascular Pathology* **1996**, 5, (2), 69-76.
25. Tekin, E.; Smith, P. J.; Schubert, U. S., Inkjet printing as a deposition and patterning tool for polymers and inorganic particles. *Soft Matter* **2008**, 4, (4), 703-713.
26. Tsai, M.-H.; Hwang, W.-S., Effects of Pulse Voltage on the Droplet Formation of Alcohol and Ethylene Glycol in a Piezoelectric Inkjet Printing Process with Bipolar Pulse. *Materials Transactions* **2008**, 49, (2), 331-338.
27. Tepe, G.; Wendel, H. P.; Khorchidi, S.; Schmehl, J.; Wiskirchen, J.; Pusich, B.; Claussen, C. D.; Duda, S. H., Thrombogenicity of various endovascular stent types: an in

- vitro evaluation. *Journal of vascular and interventional radiology : JVIR* **2002**, 13, (10), 1029-35.
28. Biggs, K. B.; Balss, K. M.; Maryanoff, C. A., Pore Networks and Polymer Rearrangement on a Drug-Eluting Stent as Revealed by Correlated Confocal Raman and Atomic Force Microscopy. *Langmuir* **2012**, 28, (21), 8238-8243.
29. Ritger, P. L.; Peppas, N. A., A simple equation for description of solute release I. Fickian and non-fickian release from non-swellable devices in the form of slabs, spheres, cylinders or discs. *Journal of Controlled Release* **1987**, 5, (1), 23-36.
30. Liggins, R. T.; Hunter, W. L.; Burt, H. M., Solid-state characterization of paclitaxel. *Journal of Pharmaceutical Sciences* **1997**, 86, (12), 1458-1463.
31. Ambike, A.; Mahadik, K. R.; Paradkar, A., Spray-Dried Amorphous Solid Dispersions of Simvastatin, a Low Tg Drug: In Vitro and in Vivo Evaluations. *Pharm Res* **2005**, 22, (6), 990-998.
32. Ishaug, S. L.; Yaszemski, M. J.; Bizios, R.; Mikos, A. G., Osteoblast function on synthetic biodegradable polymers. *Journal of biomedical materials research* **1994**, 28, (12), 1445-53.
33. Ignatius, A. A.; Claes, L. E., In vitro biocompatibility of bioresorbable polymers: poly(L, DL-lactide) and poly(L-lactide-co-glycolide). *Biomaterials* **1996**, 17, (8), 831-839.
34. Leo Slavin; Tobis, J. M., SCAI Interventional Cardiology Board Review Book. In Lippincot Williams & Wilkins a Wolters Kluwer business: 2006; p 133.
35. Porter, K. E.; Naik, J.; Turner, N. A.; Dickinson, T.; Thompson, M. M.; London, N. J., Simvastatin inhibits human saphenous vein neointima formation via inhibition of smooth muscle cell proliferation and migration. *Journal of vascular surgery* **2002**, 36, (1), 150-7.
36. Jaschke, B.; Michaelis, C.; Milz, S.; Vogeser, M.; Mund, T.; Hengst, L.; Kastrati, A.; Schömig, A.; Wessely, R., *Local statin therapy differentially interferes with smooth muscle and endothelial cell proliferation and reduces neointima on a drug-eluting stent platform*. 2005; Vol. 68, p 483-492.
37. Uurto, I.; Mikkonen, J.; Parkkinen, J.; Keski-Nisula, L.; Nevalainen, T.; Kellomäki, M.; Törmälä, P.; Salenius, J.-P., Drug-Eluting Biodegradable Poly-D/L-Lactic Acid Vascular Stents: An Experimental Pilot Study. *Journal of Endovascular Therapy* **2005**, 12, (3), 371-379.
38. Petronio, A. S.; Amoroso, G.; Limbruno, U.; Papini, B.; De Carlo, M.; Micheli, A.; Ciabatti, N.; Mariani, M., Simvastatin does not inhibit intimal hyperplasia and restenosis but promotes plaque regression in normocholesterolemic patients undergoing coronary stenting: A randomized study with intravascular ultrasound. *American Heart Journal* **2005**, 149, (3), 520-526.
39. Mikkonen, J.; Uurto, I.; Isotalo, T.; Kotsar, A.; Tammela, T. L. J.; Talja, M.; Salenius, J. P.; Törmälä, P.; Kellomäki, M., Drug-eluting bioabsorbable stents – An in vitro study. *Acta Biomaterialia* **2009**, 5, (8), 2894-2900.
40. Indolfi, C.; Cioppa, A.; Stabile, E.; Di Lorenzo, E.; Esposito, G.; Pisani, A.; Leccia, A.; Cavuto, L.; Stingone, A. M.; Chieffo, A.; Capozzolo, C.; Chiariello, M., Effects of hydroxymethylglutaryl coenzyme A reductase inhibitor simvastatin on smooth muscle cell proliferation in vitro and neointimal formation in vivo after vascular injury. *J Am Coll Cardiol* **2000**, 35, (1), 214-21.